**MDPI**

*Article*

# Allocation of Phosphorus Fractions in Chinese Fir in Response to Low Phosphorus Availability Using $^{32}$P Tracer

Xianhua Zou [1], Qingqing Liu [1], Zhijun Huang [1], Sitong Chen [2], Pengfei Wu [3], Xiangqing Ma [3] and Liping Cai [3,*]

[1] Jiangxi Provincial Key Laboratory for Restoration of Degraded Ecosystems and Watershed Ecohydrology, Nanchang Institute of Technology, Nanchang 330099, China
[2] Anhui Transportation Research Institute, Hefei 230031, China
[3] State Forestry Administration Engineering Research Center of Chinese Fir, Fujian Agriculture and Forestry University, Fuzhou 350002, China
[*] Correspondence: fjclp@126.com; Tel.: +86-0591-83780261

**Abstract:** Phosphorus (P) is among the most intractable constraints on plant fertility, particularly in acidic soils with high P fixation capacities. The effects of nutrient limitation and the adaptive strategies of plants in infertile soils are central topics in plant ecology. The development of tree cultivars with greater P use efficiency (PUE), defined as the ability of a tree to grow and be productive in soils with reduced P availability, would substantially improve forest development. The ability of plants to redistribute and transfer P across fractions determines their adaptability to P limitations. However, the mechanisms of P utilization and transport remain unknown in Chinese fir (*Cunninghamia lanceolata* (Lamb.) Hook.) from the perspective of P fraction distribution. In this study, we investigated the distribution and translocation patterns of exogenous P and different P fractions in the M1 Chinese fir, which was identified as exhibiting high P-deficient resistance ability and maintaining higher yield under low P stress relative to the average clones, using $^{32}$P tracking, which can accurately trace the migration pathways of exogenous P after plant absorption. We found that exogenous P in the roots was higher than in the stems or leaves under low-P conditions in which the amount of the exogenous P absorbed by M1 was significantly reduced. Under low-P conditions, the plants optimized P allocation, which led to higher PUE than under high-P conditions, with the highest PUE in the leaves, followed by the stems and roots. The M1 clone maintained a high ratio of soluble P (i.e., inorganic P and ester P) in its leaves and stems, which improved P mobility and recycling under the conditions of limited P. In the roots, the P fractions shifted from soluble inorganic P and ester P to insoluble P (i.e., nucleic P), but the total P concentration was relatively stable, which may ensure root growth and exogenous P absorption under the conditions of limited P. Our results confirm that the M1 Chinese fir reduces P demand, optimizes the allocation of P among P fractions, and increases PUE to maintain aboveground productivity in response to limited P conditions.

**Keywords:** Chinese fir; P fractions; high- and low-P treatments; isotopic tracking

## 1. Introduction

Plant nutritional acquisition strategies and their underlying mechanisms have long been fundamental topics in ecology [1]. P is one of six macronutrients essential for plant growth and development due to its function in genetic material, in free nucleotides for energy transfer, in phospholipids as membrane components, and in carbon metabolism as sugar phosphates [2]. However, P is a common limiting nutrient of productivity in plants [3] due to its low soil mobility and precipitation with other soil minerals, such as iron (Fe) and aluminum (Al) in acidic soils and calcium (Ca) in alkaline soils [4,5]. The development of forest cultivars with greater PUE, defined as the productivity per unit of absorbed P, would substantially improve forestry development [6,7].

P utilization in plants is affected by a series of physiological, structural, and growth characteristics [8]. With the low availability of soil P, plants can increase PUE by reducing

metabolic activities and increasing P reuse [9]. One method considered to be an effective way to improve PUE is adjusting the concentration and ratios of different P fractions in plants [10]. Plants can accumulate both organic and inorganic P; inorganic P is composed of metabolic P and stored P [11], while organic P primarily forms the structural material of most cell membranes [12]. It has been shown that P is divided between nucleic, ester, and lipid forms [13,14]. Ester P and some inorganic P are actively metabolized by plant cells and are highly soluble, and the decomposition of ester P in cells is fundamental to energy and material metabolism. To some extent, the amount of nucleic P can reflect the activity of plant protein synthesis and metabolism [15]. Lipid P is insoluble and lineages with high PUE tend to reduce insoluble and less-soluble P fractions while increasing the proportion of soluble inorganic P to enhance its mobility [16]. The composition and distribution of P fractions in plant tissues may also be affected by the plant's P nutritional status. P deficiency generally decreases the amount and proportion of inorganic P, and organic P becomes the main P pool in plants [7,10]. It has been reported that the ability of plants to redistribute and transfer P fractions affects their adaptability to P limitation [17,18]. However, previous studies mainly focused on leaf responses or herbaceous plants [12,18,19], and few studies have tracked the distribution and translocation of P fractions in woody plants in multiple organs over time.

The Chinese fir (*Cunninghamia lanceolata* (Lamb.) Hook.) is one of the main species used for afforestation in southern China, but continuous planting and decreased soil fertility have led to reduced productivity. The low soil availability of P resulting from strong P fixation in acidic soils is an important factor contributing to reductions in productivity [20]. Our previous studies have identified some Chinese fir clones that had high yields despite low soil P concentrations relative to the average clones [21]. The response mechanisms of these Chinese fir clones to P deficiency have also been investigated in our preliminary studies [22–26]. These studies showed that increasing acid phosphatase activity in leaves and roots was an important adaptive mechanism for P deficiency [27,28]. Acid phosphatase is an important enzyme that regulates P metabolism in biological cells and exists widely in plant organs. It can release inorganic P by degrading some organic P compounds and plays an important role in the absorption, activation, and reuse of P in plants [29]. It was reported that *Hordeum vulgare* L. with high PUE could enhance the decomposition of ester P and nucleic P by increasing the activity of acid phosphatase in leaves and converting them to inorganic P to increase the proportion of mobile P, so as to improve P reutilization at a later growth stage [30]. We hypothesize that the Chinese fir clones, which showed higher acid phosphatase activity, adapted to P-deficient conditions by adjusting the concentration and ratios of different P fractions to affect the plant's P nutritional status. The high yields of these Chinese fir clones may also result from the redistribution and translocation of P fractions in trees under low soil P conditions.

To investigate the above hypotheses, we selected the M1 Chinese fir clone as our research subject. This clone maintained high productivity, demonstrated by a biomass increase of 32.60% in P-deficient conditions, compared with the conditions of normal P concentration, while the biomass in 20 other Chinese fir clones decreased by 31.97% on average in P-deficient conditions [21]. We investigated the distribution and translocation of different P fractions in the M1 clone after exogenous P uptake under low-P supply, after chemically separating plant P into the following major fractions: inorganic P and three classes of organic P (lipid, nucleic, and ester). In order to accurately trace the migration pathways of exogenous P after absorption into the plant, we selected the $^{32}$P radioisotope technique [31,32], and four monitoring times (0.5d, 1d, 5d, and 15d) were set to capture the dynamics of exogenous P and the different P fractions in multiple organs under different levels of P supply. We also calculated the PUE of multiple organs and examined the relationships among the different P fractions and PUE. We aimed to comprehensively explore P utilization in the M1 Chinese fir from the perspective of P fraction distribution and translocation to identify the mechanisms underlying the plant's maintained yield under

conditions of low P and provide a new empirical basis for the breeding of P-use-efficient plant genotypes.

## 2. Materials and Methods

### 2.1. Plant Material

The experiment was carried out using a Chinese fir clone M1 that was identified in a preliminary study as exhibiting high yields despite low soil P concentrations relative to the average clones [21]. The plantlets of the clone were raised through reproductive cloning and were cultivated in the Wuyi State-owned Forest Farm, Zhangping, in Fujian Province, People's Republic of China. The plantlets were cultivated in a greenhouse with an average temperature of 20.3 °C and relative humidity was 78%, and the cultivation medium was a mixed substrate with a 20-20-40 ratio of peat soil, perlite, and Chinese fir skin. The plantlets were watered 3–4 times weekly. One-year-old healthy plantlets were chosen for the experiment, with a height of $17.5 \pm 0.2$ cm and a stem diameter of $2.30 \pm 0.05$ mm at the beginning of the experiment.

### 2.2. Study Design

The experiment was conducted in the Isotope Laboratory of the College of Sciences, Nanjing Agricultural University. The plants were grown in polyethylene containers (4.5 cm diameter, 30 cm depth) in a hydroponic culture to optimize the absorption of exogenous P. Each seedling was wrapped with a sponge and fixed at the mouth of the container in a polyethylene foam plate with a 2 cm diameter seedling hole cut in the middle of the foam plate. The stem–root transition zone of each seedling was wrapped in sponges and fixed in the seedling hole. One air hole was drilled in each polyethylene container and connected to the ventilation pump with a ventilation tube. During the experiment, a 20 min ventilation process controlled by an automatic timer was performed every 4 h to ensure a sufficient oxygen supply to the plantlets, and the rate of gas flow was 26.5 m$^3$ h$^{-1}$. The average temperature in the greenhouse was 25 °C, with a 14:10 h (day:night) photoperiod and relative humidity > 80%.

The plantlets were divided between two P concentration conditions, high-P and low-P, with P concentrations set according to the soil available P in southern Chinese fir plantation forests measured by Sheng and Fan [33], who showed that the optimum available P in southern Chinese fir forests was 13 mg kg$^{-1}$ (high-P) and the limiting value was 1 mg kg$^{-1}$ (low-P). We used KH$_2$PO$_4$ as the source of P, and high- and low-P treatments were 0.50 mmol L$^{-1}$ KH$_2$PO$_4$ and 0.03 mmol L$^{-1}$ KH$_2$PO$_4$, respectively. The potassium (K) levels of the nutrient solutions used in the different treatments were adjusted with KCl during the experiment based on the modified Hoagland formula of Wu et al. [34]: 127.5 mg L$^{-1}$ KNO$_3$,122.5 mg L$^{-1}$ MgSO$_4$·7H$_2$O, 294.92 mg L$^{-1}$ Ca(NO$_3$)$_2$·4H$_2$O, trace elements (0.71 mg L$^{-1}$ H$_3$BO$_3$, 0.02 mg L$^{-1}$ CuSO$_4$·5H$_2$O, 0.055 mg L$^{-1}$ ZnSO$_4$·7H$_2$O, 0.4525 mg L$^{-1}$ MnCl$_2$·4H$_2$O, and 0.015 mg L$^{-1}$ H$_2$MO$_4$·4H$_2$O), and an iron salt solution (1.393 mg L$^{-1}$ FeSO$_4$·7H$_2$O and 1.863 mg L$^{-1}$ Na$_2$EDTA). The pH of the nutrient solution was regulated to 5.5 with NaOH and diluted HCl: NaOH was selected when the pH of the nutrient solution was lower than 4.5, and HCl was used when the pH was higher than or equal to 4.5.

$^{32}$P is an ideal radionuclide for use in plant physiology and fertilization studies due to its nuclear features [35]: It is a pure beta emitter with the maximum β$^-$ radiation energy E$_{max}$ = 1.7 MeV and a half-life of 14.3d. Based on these properties, we assessed the plant's P concentration at four time points during the experiment (0.5d, 1d, 5d, and 15d). We prepared the $^{32}$P radioactive solution using a stock solution of $^{32}$P-orthophosphate with a radioactive concentration of $4.05 \times 10^4$ Bq mL$^{-1}$ (PerkinElmer, Boston, MA, USA). Each single seedling pot contained 250 mL of the nutrient solution and 650 μL of the $^{32}$P-orthophosphate solution. The specific activity (the ratio of radioactivity to P content) rates of high-P and low-P treatments were 6.81 Bq μg$^{-1}$ and 113.45 Bq μg$^{-1}$, respectively. The calculated method is shown in Equation (2). In addition, $^{32}$P decays under natural

conditions, so we also prepared five polyethylene containers without plantlets for each nutrient solution (i.e., high- and low-P concentrations) and $^{32}$P-orthophosphate solution, and they were used as blanks to determine the specific activity at the end of the experiment. This decay reading was subtracted when calculating the actual amount of P absorbed by the plantlets. There were 5 replicates for each treatment, for a total of 40 plantlets, in this study.

### 2.3. Determination Methods

#### 2.3.1. Determination of Dry Weight

At harvest time, the roots were rinsed with distilled water until the radioactivity of $^{32}$P on the root surface was less than the detection limit of a liquid scintillation counter (LSC; Beckman LS6500) (Beckman, Brea, CA, USA). The plants were separated into individual plant parts, i.e., roots, stems, and leaves. For the determination of the radioactivity level of the different organs, new lateral roots were collected 15 mm from the root tip, which represented the strongest nutrient absorption capacity. The 4th to 10th leaves as well as the stems between them were collected as leaf and stem samples, respectively. The fresh samples of each organ were placed into liquid nitrogen, freeze-dried, and then ground. The samples were stored at $-80$ °C for radioactivity determination (below). The other plant material was dried at 105 °C for 2 h and then at 75 °C to a constant mass and measured for oven-dried mass. We analyzed the impact on the growth of plantlets by calculating the difference in dry mass increase before and after treatments.

#### 2.3.2. Radioactivity Determination of Total Exogenous P and Different P Fractions in Plantlets

We divided the plant's P concentration into four fractions: inorganic P, lipid P, ester P, and nucleic P. The fractionation procedure was based on sequential extraction [36], with some modifications [12]. For each plant, 0.03 g freeze-dried and ground samples of each organ (root, stem, and leaf) were weighed for the radioactivity determination of the total exogenous absorbed P. We also separately weighed 0.20 g samples of root, stem, and leaf, ground them into homogenates, and rinsed them with 4 mL of 5% trichloroacetic acid (TCA) in centrifuge tubes. Then, 1 mL of 5% TCA was added, and the samples were centrifuged at $1180\times g$ for 5 min. We transferred the resulting supernatants into 25 mL volumetric flasks, added 5 mL acetone, shook well, added 5 mL ammonium molybdate reagent, mixed, allowed the mixtures to rest for a few minutes, and then transferred them into separatory funnels. We then added 10 mL of a water-saturated mixture of isobutanol and benzene to each sample and shook vigorously. After resting for a few minutes, the solutions separated into two layers: an acidic inorganic P (Pi) bottom layer and an organic P compound upper layer. We collected the two layers in 25 mL volumetric flasks containing distilled water for Pi and acetone for organic P. After the main component of the organic P solution (ester P) was removed, we extracted the residue with 3 mL of 95% ($w/v$) ethanol. We continued to extract with a total of 3 mL 2:1 mixed solution (ethanol and ether, $v/v$) after allowing the solution to sit for 10 min and centrifuging at $1089\times g$ for 8 min. Each extraction resulted in a lipid P supernatant, and the extraction solution was adjusted to 25 mL with acetone. The precipitate was hydrolyzed with 5 mL of 0.5 mol KOH at 36 °C for 18 h and cooled, after which $MgCl_2$ was added to accelerate RNA decomposition and acidified to pH = 1 with 72% $HClO_4$ before centrifuging at $1180\times g$ for 10 min. The resulting supernatant contained P-RNA, and the volume was fixed to 25 mL with distilled water. A final precipitate was extracted by adding 5 mL of 5% $HClO_4$ and incubating it at 90 °C in a water bath for 15 min. The solution was separated into two layers after centrifuging at $1180\times g$ for 10 min, and a supernatant containing P-DNA was extracted and brought to 25 mL with distilled water.

The above extraction steps were repeated four times for complete separation, and the final P fractions were determined uniformly. All samples were decolorized and filtered with activated carbon, and then 1 mL was pipetted, and the radioactivity of the samples was determined using a liquid scintillation counter (Beckman LS6500) (Beckman, Brea, CA,

USA) after adding scintillation liquid (PerkinElmer, Boston, MA, USA) for 12 h. The data obtained from LSC were transformed into units of disintegration per minute (dpm) by dividing cpm by LSC efficiency: dpm = cpm/efficiency [37]. The data were recorded as the averages of five replicates. The reference moment chosen for all activity results was the harvesting time. $^{32}$P uptake was calculated using the following decay correction:

$$A = A_0 e^{-\lambda t} \tag{1}$$

where A is the remaining activity of $^{32}$P after decay at time t (from the measurement time to the reference time), $A_0$ is the activity of $^{32}$P at t = 0, and $\lambda$ is the decay constant of $^{32}$P. The formula for calculating $\lambda$ is $\lambda = \ln 2/T_{1/2}$, where $T_{1/2}$ is the half-life of $^{32}$P, which is 14.3d.

### 2.3.3. Determination of Specific Activity

Specific activity, expressed in units of Bq $\mu g^{-1}$, was defined as the ratio of radioactivity to P content in the solutions (see Section 2.2. Study Design, above) and calculated as follows:

$$SA = \frac{R_l}{m_p} \tag{2}$$

where SA is the specific activity, $R_l$ is the radioactivity of the nutrient solution, and $m_p$ is the P content in the nutrient solution.

### 2.4. Data Analyses

We calculated the content of exogenous P of each organ on a dry matter basis by dividing the radioactivity of each organ by the specific activity and dry mass:

$$M_{TP} = \frac{R_{TP} * \frac{1}{SA}}{m_0} \tag{3}$$

where $M_{TP}$ (expressed in units of $\mu g\ g^{-1}$) is the content of exogenous P of each organ on a dry matter basis, $R_{TP}$ (expressed in units of Bq) is the radioactivity of exogenous P absorbed in each organ, SA (expressed in units of Bq $\mu g^{-1}$) is the specific activity (Equation (2)), and $m_0$ (expressed in units of g) is the dry mass of each organ. Equation (3) was also used to calculate the content of each P fraction in each organ, which was calculated similarly.

We also calculated the distribution ratio of the different P fractions in each organ to the total exogenous P absorbed in the plant; the distribution ratio ($r_{FP}$, %) was calculated as follows:

$$r_{FP} = \frac{M_{FP}}{M} \times 100\% \tag{4}$$

where $r_{FP}$ is the distribution ratio of a given P fraction in a given each organ, $M_{FP}$ is the content of that P fraction in the organ on a dry matter basis, and M (expressed in units of $\mu g\ g^{-1}$) is the content of that total P in the plant, which is calculated as the sum of $M_{TP}$ in the different organs.

Finally, we calculated the PUE (g $\mu g^{-1}$) of each organ, to investigate the amount of total biomass that was produced per unit of P taken up in each organ.

Statistical analyses were performed in SPSS version 19.0 (SPSS Inc., Chicago, IL, USA), and graphs were plotted using Origin 8.5 (Origin Lab Corporation, Northampton, MA, USA). Paired *t*-tests were used to compare the differences between high- and low-P treatments at each time point. One-way ANOVA was used to evaluate the differences between the time points for the total P concentrations, distribution ratios, relative proportions of each P fraction, and PUE. Pearson correlation analysis was used to examine the relationships among the different P fractions and PUE. All tests were performed using a confidence level of $p < 0.05$. We further investigated significant effects with Duncan's multiple-range test at a 5% significance level to test for differences between treatments.

## 3. Results

### 3.1. Comparison of the Increase in Dry Weight after Different P Treatments

We observed almost no increase in dry weight at 0.5d and 1d, likely because of the short treatment time (Figure 1). The dry weight of the different organs slightly increased during treatment for 5 days; however, the influence of the different P treatments on the growth of M1 was not obvious. After 15 days, a significant difference was observed in the dry weight between low-P and high-P treatments. The increase in the dry weight of the whole plant under the low-P treatment was about 3.6 times higher than that under the high-P treatment; specifically, the increase in roots, stems, and leaves under the high-P treatment was only 42.27%, 26.48%, and 19.62% of low-P conditions, respectively. We, therefore, concluded that the M1 clone showed higher productivity under the low-P treatment than under the high-P treatment when the treatment time was extended to 15d.
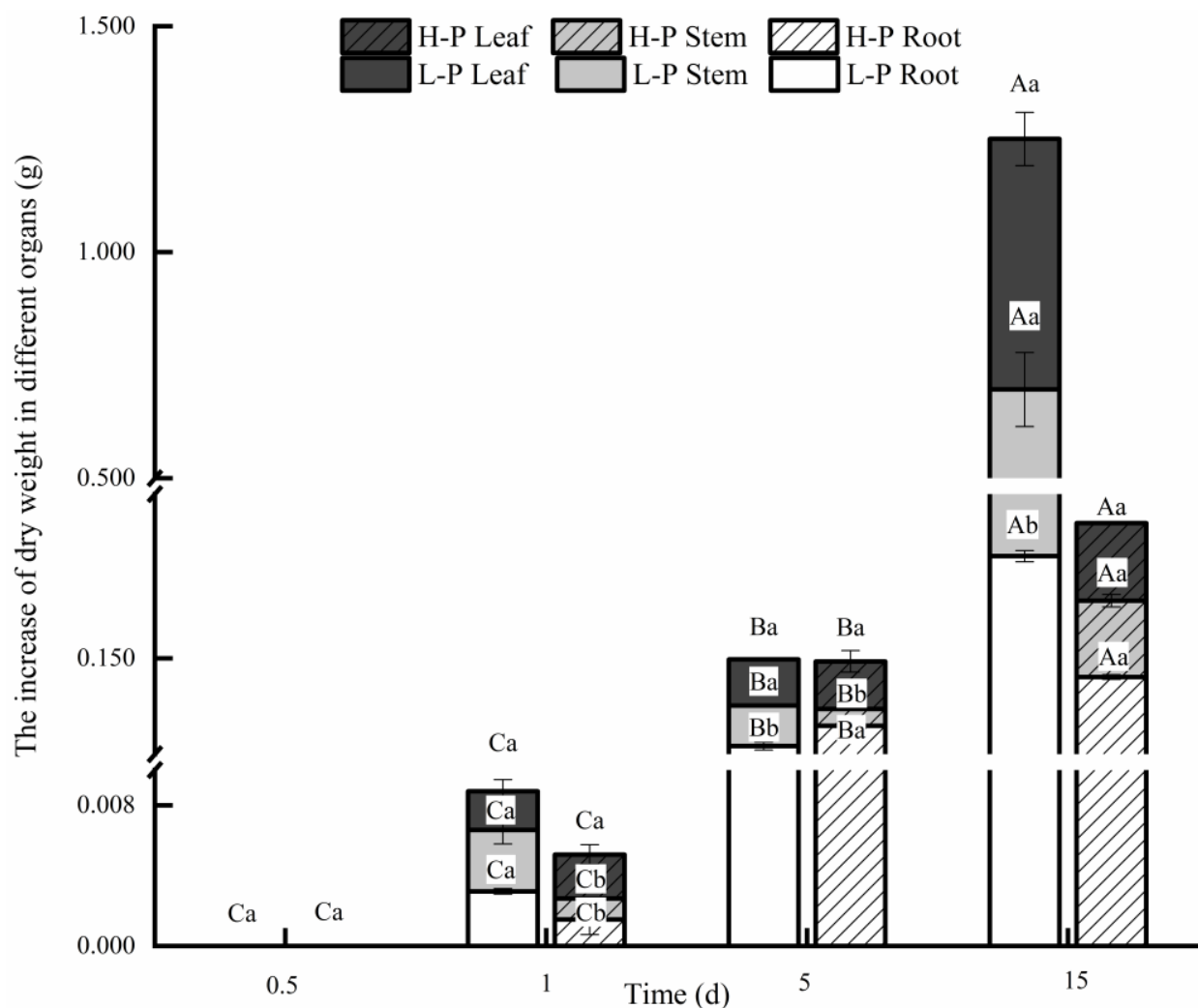


**Figure 1.** The increase in dry weight in different organs at different treatment times under different P supply conditions. "L-P" and "H-P" represent the low-P and high-P treatments, respectively. Error bars represent standard error, and each point in the figures represents the mean of five replicates (*n* = 5). Lowercase letters indicate significant differences (*p* < 0.05) at different treatment times under the same P treatment. Uppercase letters indicate significant differences (*p* < 0.05) between different treatments at each time point. Labeling conventions are the same across time points.

### 3.2. Comparison of Exogenous P Distributions after Different P Treatments

The distribution of exogenous P in the roots was significantly higher than in the leaves and stems (Figures 2 and S1). The concentration of exogenous P in the leaves and stems

only reached 7.7%–10.5% of that in the roots under the different P supply conditions after 15 days. A comparison of high- and low-P treatments showed that the concentration of exogenous P contained in the plants under the low-P treatment was significantly lower than that of the plants under the high-P treatment ($p < 0.05$). The differences were initially quite small, but the P uptake under the high-P treatment increased sharply from 5d to 15d. The amount of the exogenous P contained in the roots under the low-P treatment at 5d and 15d was only 13.3% and 4.8% of that of the roots under the high-P condition, respectively.
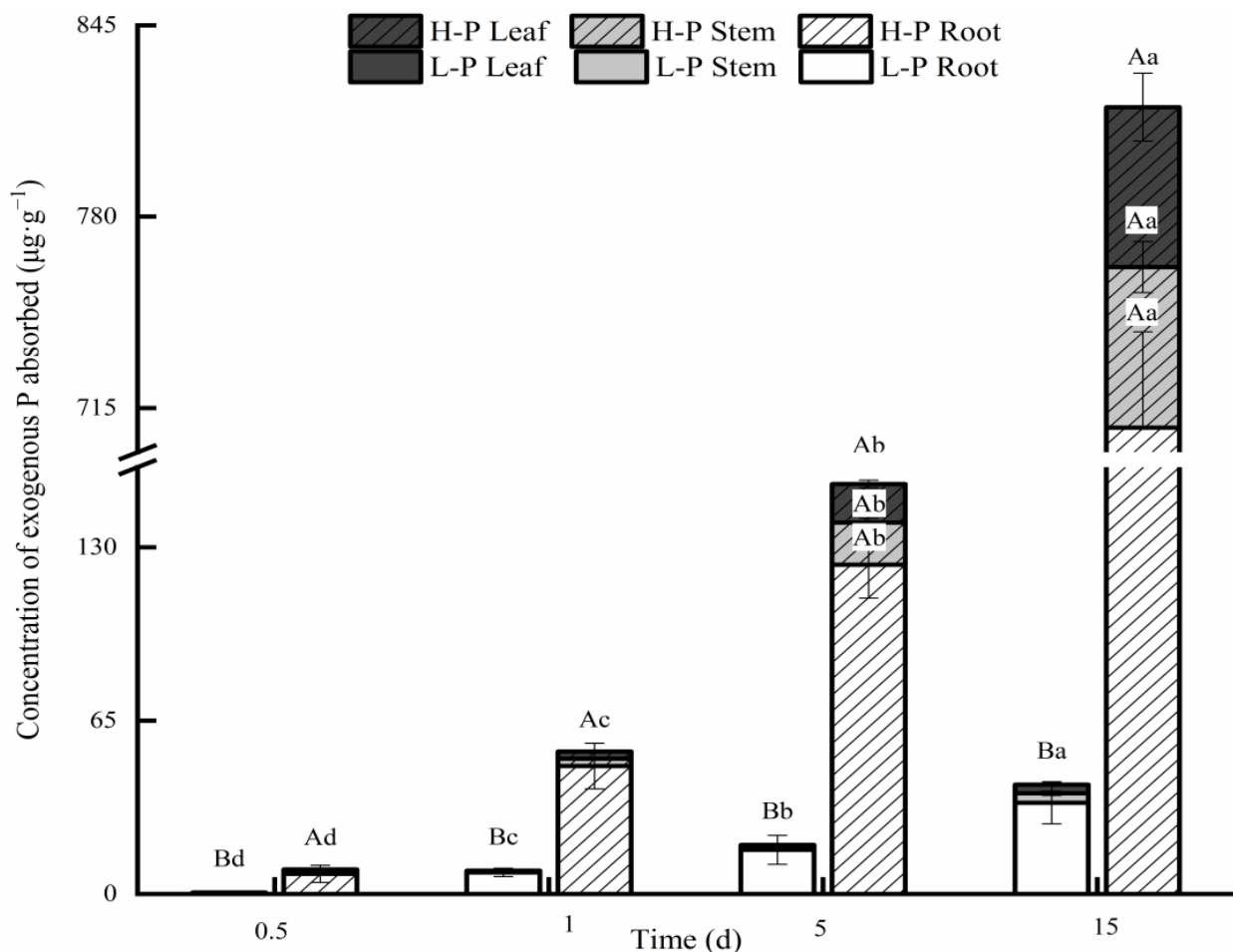


**Figure 2.** The concentration of exogenous P in different organs of M1 Chinese fir under different P supply conditions. "L-P" and "H-P" represent the low-P and high-P treatments, respectively. Error bars represent standard error, and each point in the figures represents the mean of the five replicates ($n = 5$). Lowercase letters indicate significant differences ($p < 0.05$) at different treatment times under the same P treatment. Uppercase letters indicate significant differences ($p < 0.05$) between treatments at each time point. Labeling conventions are the same across time points.

The ratios of the exogenous P absorbed in the different organs showed that the roots absorbed the most exogenous P (80%–90%), followed by the stems and leaves, regardless of the P treatment (Figure 3). The ratio of the exogenous P in the aboveground organs initially decreased over the first day but increased in both treatments over 5d and 15d. The ratios of the root, stem, and leaf P were similar in high- and low-P treatments at 0.5d ($p > 0.05$), but the P ratios of the leaves and stems decreased under the low-P treatment relative to the high-P treatment ($p < 0.05$). The ratios of the stem P under the low-P treatment were 59.4% and 75.2% of those under the high-P treatment after 5d and 15d, and the ratios in the leaves were similarly low. In contrast, the ratio of P in the roots was higher under the low-P treatment than under the high-P supply from 1d to 15d.
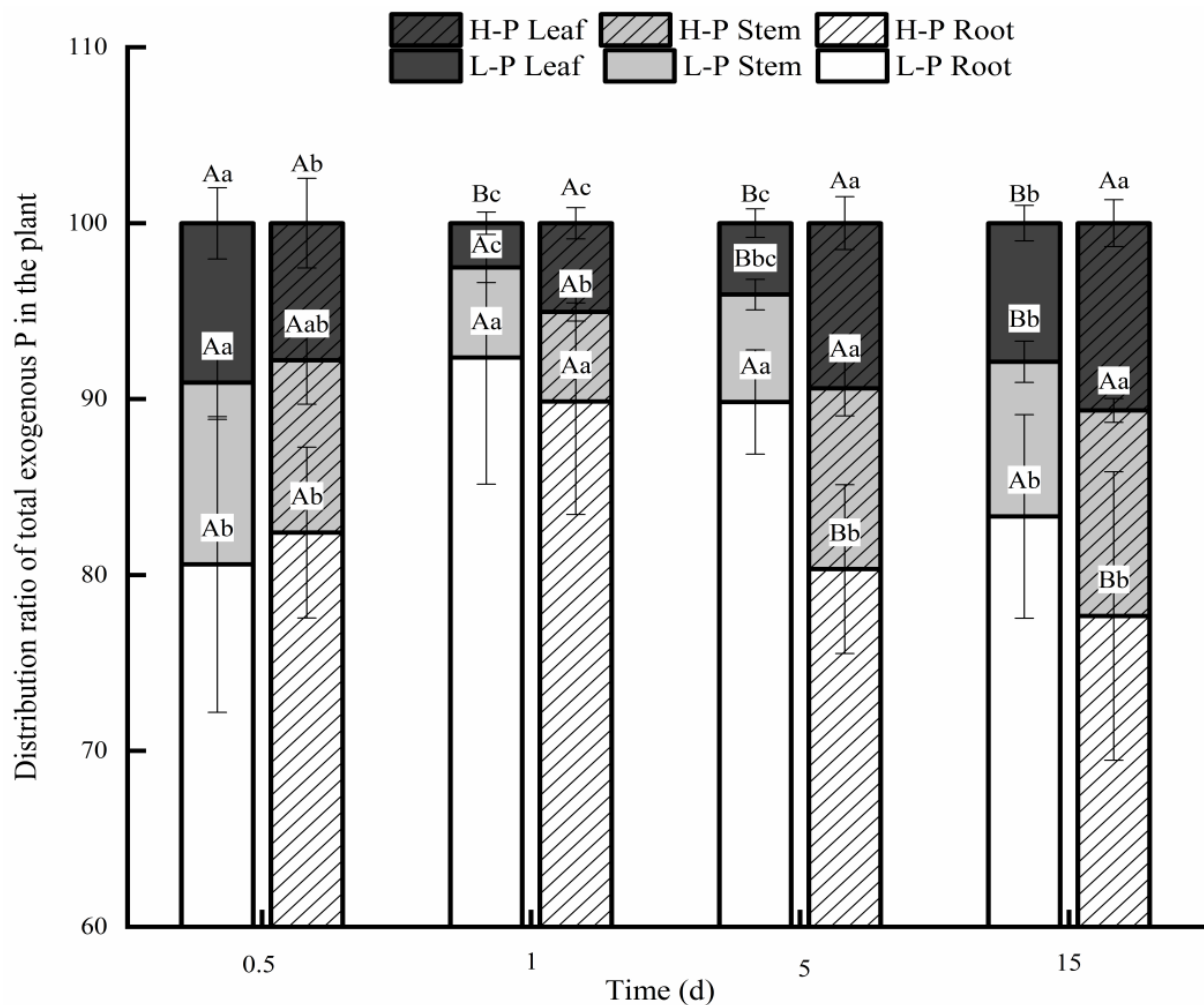
**Figure 3.** The distribution ratio of exogenous P absorbed in different organs of M1 Chinese fir under different P supply conditions. "L-P" and "H-P" represent the low-P and high-P treatments, respectively. Lowercase letters indicate significant differences ($p < 0.05$) at different treatment times under the same P treatment. Uppercase letters indicate significant differences ($p < 0.05$) between different treatments at each time point.

### 3.3. Distribution of P Fractions in Leaves under Different P Treatments

We calculated the ratio of the different P fractions in each organ to the total exogenous P absorbed in the plant for presenting the distribution pattern of the different P fractions.

The contents of P fractions at 0.5d in the leaves under both conditions were lower than the detection limit, which we recorded as 0 μg g$^{-1}$ (Figure 4). We found that the distributions of inorganic P and ester P in the leaves were similar between high- and low-P treatments. Under the high-P supply, the ratios of inorganic P and ester P peaked at 5d before significantly decreasing at 15d ($p < 0.05$; Figure 4A,B). Under the low-P treatment, the ratios of inorganic P and ester P in the leaves increased throughout the experiment, and the ratios after 15d were significantly higher than the ratios of all earlier time points ($p < 0.05$; Figure 4A,B), and both were higher than those of the high-P treatment. The ratio of soluble P remained high in the leaves of M1 Chinese fir under the low-P treatment. The lipid-P content in the leaves increased over 5d in both high- and low-P conditions and remained stable between 5d and 15d (Figure 4C). The ratios of lipid P under the low-P treatment decreased relative to the high-P treatment ($p < 0.05$) at 5d and 15d, when the ratio was significantly higher than that of the high-P treatment at 1d ($p < 0.05$). Similarly, the ratio of nucleic P in the leaves increased up to 5d and remained stable from 5d to 15d under high-P supply, while the proportion of nucleic P in the leaves continuously increased under

the low-P treatment (Figure 4D). In the low-P treatment, the nucleic-P ratio at 15d was four-fold higher than that of 1d and was significantly higher than that under the high-P supply ($p < 0.05$).
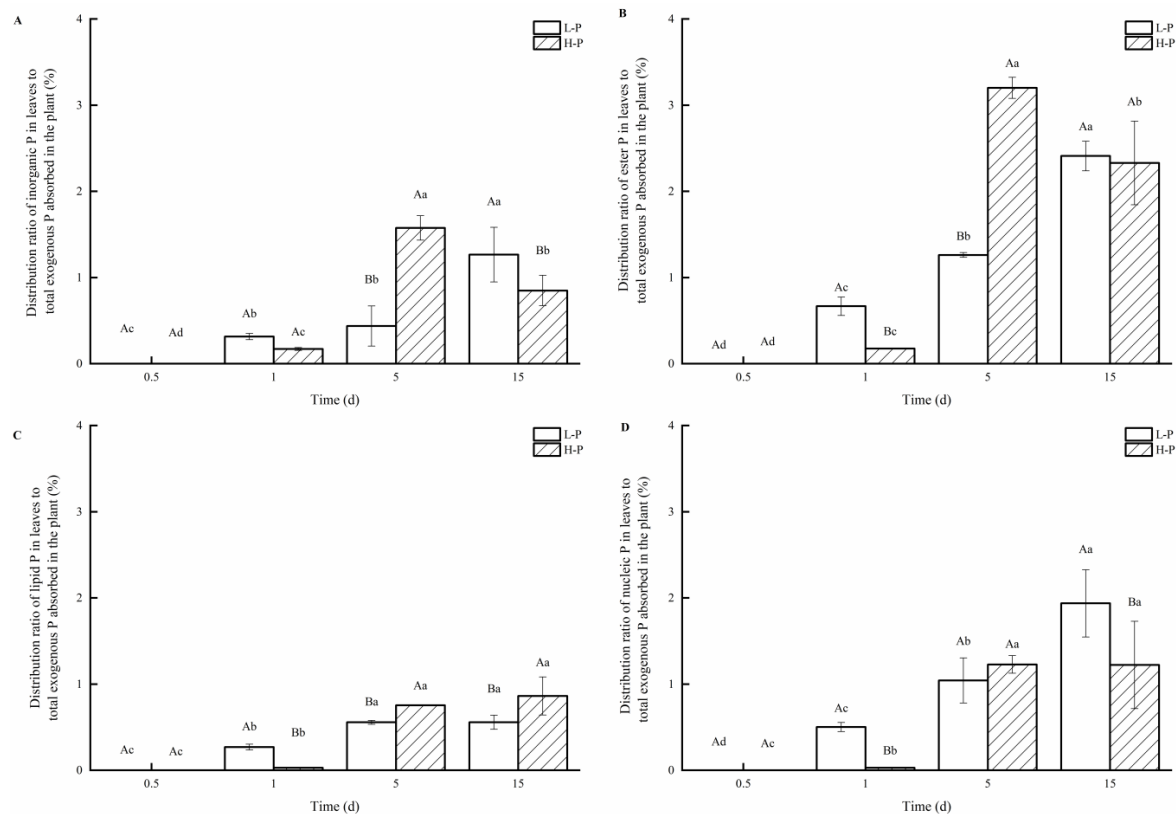


**Figure 4.** Percentage of different P fractions in leaves to total exogenous P absorbed in the plant under high- and low-P treatments: (**A**) inorganic P, (**B**) ester P, (**C**) lipid P, and (**D**) nucleic P. "L-P" and "H-P" represent the low-P and high-P treatments, respectively. Error bars represent standard error, and each point in the figures represents the mean of the five replicates (*n* = 5). Lowercase letters indicate significant differences ($p < 0.05$) at different treatment times under the same P treatment. Uppercase letters indicate significant differences ($p < 0.05$) between different treatments at each time point.

### 3.4. Distribution of P Fractions in Stems under Different P Treatments

As in the leaves, the stem P fractions at 0.5d were below the detection limit and were recorded as 0 µg g$^{-1}$ (Figure 5). The distribution of inorganic P and ester P in the stems was similar to what was observed in the leaves (Figure 5A,B). The proportions of inorganic P and ester P to the total exogenous P absorbed in the plant were also higher under the low-P treatment at 15d, with the ratio of inorganic P under low-P conditions being twice that under high-P conditions. The amount of soluble P in M1 stems also remained high-under low-P treatments. Like the leaves, there was no significant difference between the lipid-P ratios in the stems under the different P treatments ($p > 0.05$), but lipid P slightly increased by 15d under the low-P treatment (Figure 5C). The ratio of nucleic P in the stems was also similar to the ratio in the leaves: the proportion of nucleic P in the stems increased until 5d and was stable from 5d to 15d under the high-P supply, while the proportion of nucleic P in the stems continuously increased under the low-P supply (Figure 5D).
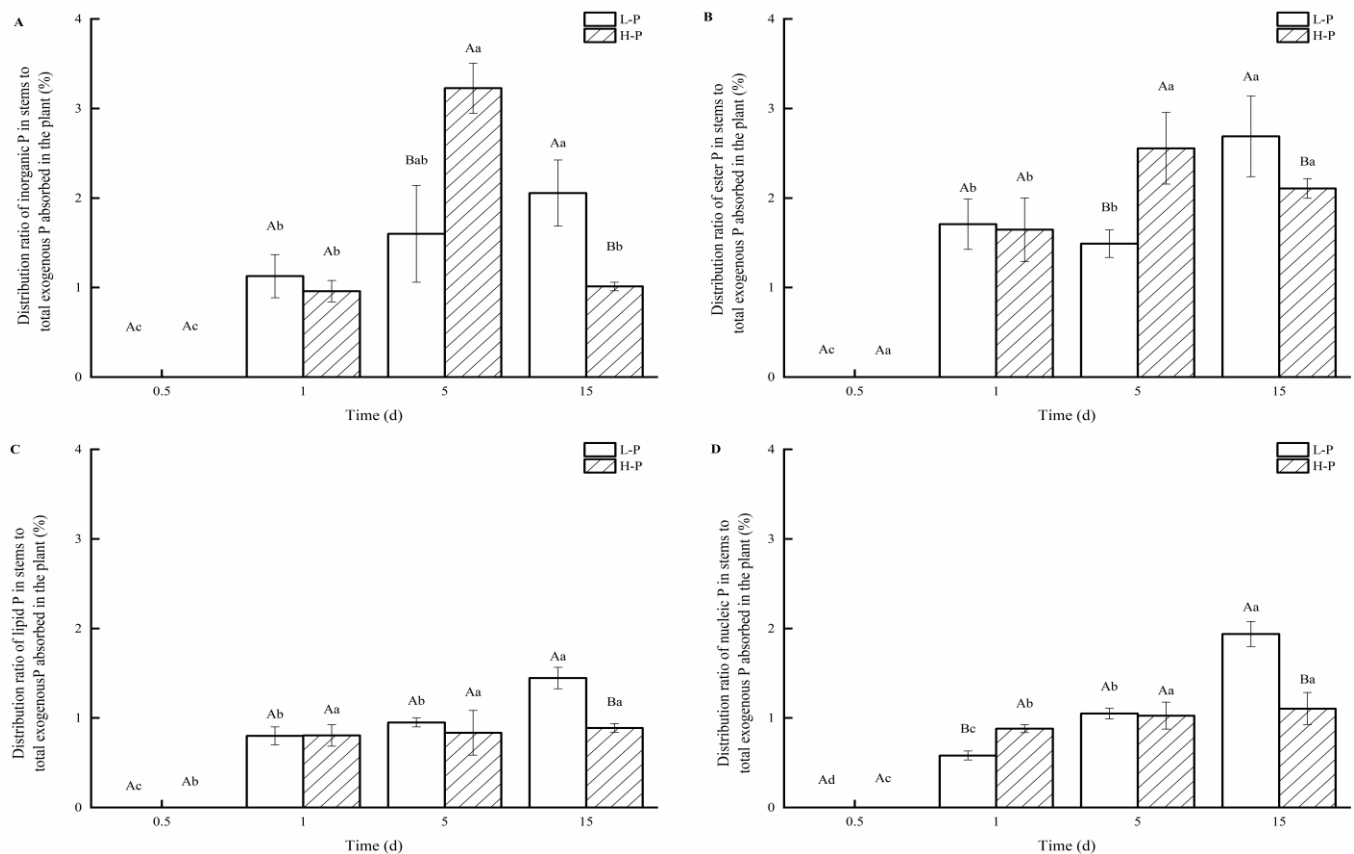
**Figure 5.** Percentage of different P fractions in stems to total exogenous P absorbed in the plant under high- and low-P treatments: (**A**) inorganic P, (**B**) ester P, (**C**) lipid P, and (**D**) nucleic P. "L-P" and "H-P" represent the low-P and high-P treatments, respectively. Error bars represent standard error, and each point in the figure represents the mean of the five replicates ($n = 5$). Lowercase letters indicate significant differences ($p < 0.05$) at different treatment times under the same P treatment. Uppercase letters indicate significant differences ($p < 0.05$) between different treatments at each time point.

*3.5. Distribution of P Fractions in Roots under Different P Treatments*

The changes in inorganic P and ester P in the roots were different from the trends in the leaves and stems. Regardless of the P treatment, inorganic P in the roots generally decreased over the course of the experiment (Figure 6A), while ester P peaked at 1d and was not significantly different between 0.5d, 5d, and 15d (Figure 6B). The ratios of inorganic P and ester P were also lower under the low-P treatment than those under the high-P treatment from 0.5d to 15d, and the differences at most time points were significant ($p < 0.05$; Figure 5A,B). We did not observe any changes in the ratios of lipid P in the roots of either P treatment ($p > 0.05$; Figure 6C), but lipid P was slightly decreased in the low-P treatment. The patterns of the roots' nucleic P ratios were markedly different between high- and low-P treatments. Under the high-P supply, the ratio of nucleic P was constant over time ($p > 0.05$), while the ratio of nucleic P significantly increased with time under the low-P treatment (Figure 6D). The ratio of nucleic P in the roots at 15d was higher than that at 0.5d under the low-P treatment. Moreover, in contrast to the root's inorganic P, ester P, and lipid P, all ratios of nucleic P were higher in the low-P treatment than those in the high-P supply over the course of the experiment.
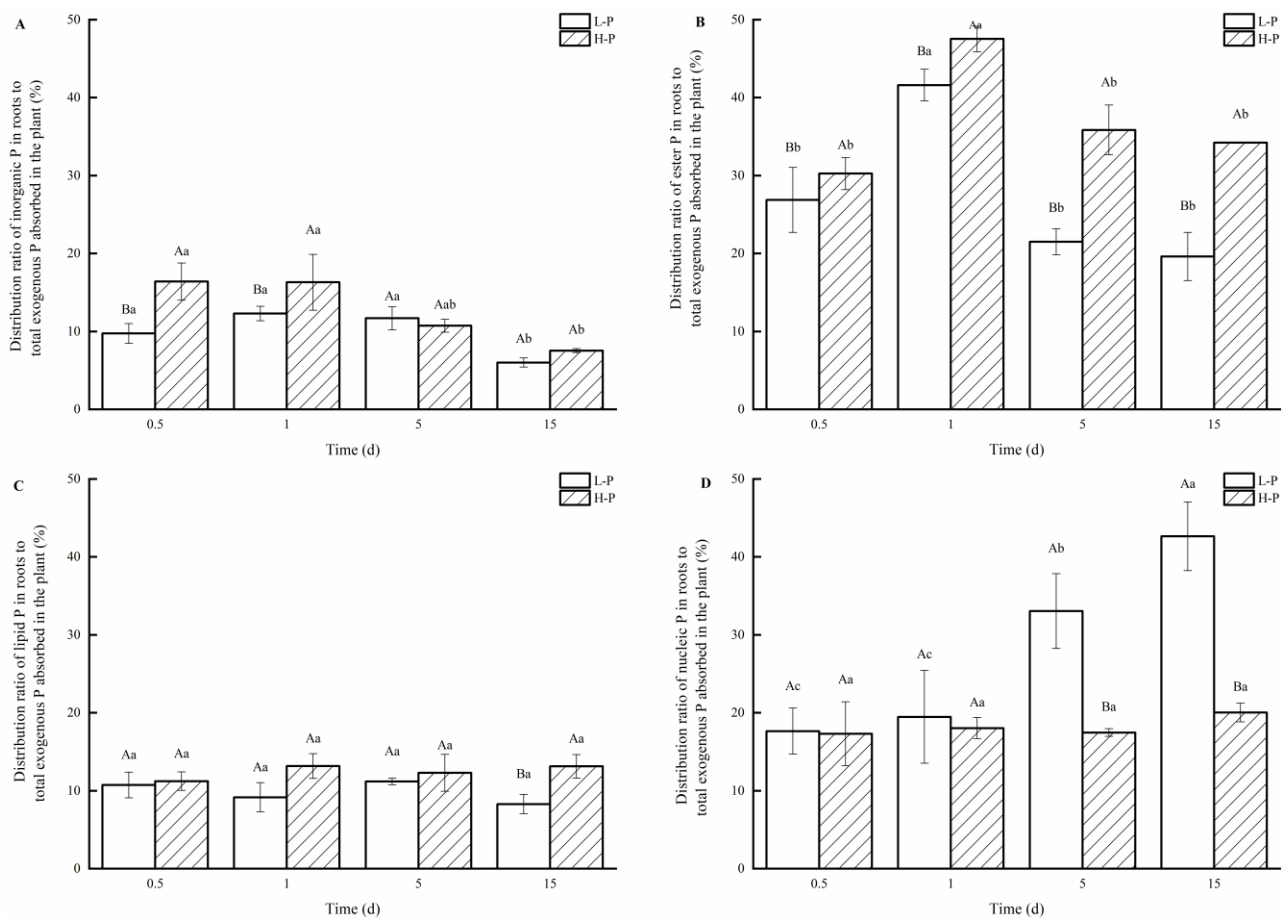
**Figure 6.** Percentage of different P fractions in roots to total exogenous P absorbed in the plant under high- and low-P treatments: (**A**) inorganic P, (**B**) ester P, (**C**) lipid P, and (**D**) nucleic P. "L-P" and "H-P" represent the low-P and high-P treatments, respectively. Error bars represent standard error, and each point in the figures represents the mean of the five replicates (*n* = 5). Lowercase letters indicate significant differences (*p* < 0.05) at different treatment times under the same P treatment. Uppercase letters indicate significant differences (*p* < 0.05) between different treatments at each time point.

### 3.6. PUE in Different Organs under Different P Treatments

The PUE was highest in each organ at 0.5d (*p* < 0.05) under both high- and low-P treatments (Figure 7). The PUE of each organ slightly decreased from 1d to 15d under the low-P treatment, but there was no significant difference between the time points (*p* > 0.05). The PUEs of leaves, stems, and roots at 15d under and the low-P treatment were all lower than those at 0.5d. Similarly, under high-P conditions, the PUE of each organ decreased from 0.5d to 1d and then remained stable. The leaf PUE was the highest, followed by the PUE of the stems and roots, regardless of the P treatment. The PUE of the leaves was nearly 9 times that of the roots at 0.5d under the low-P treatment and reached more than 10 times higher under the high-P treatment. A comparison of high- and low-P treatments at each time point showed that the PUE of each organ under the low-P treatment was significantly higher than those observed under the high-P treatment at each time point (*p* < 0.05). For example, the PUEs of the leaves, stems, and roots at 0.5d under the high-P treatment were only 6.90%, 6.24%, and 5.70% of those under the low-P treatment, respectively.
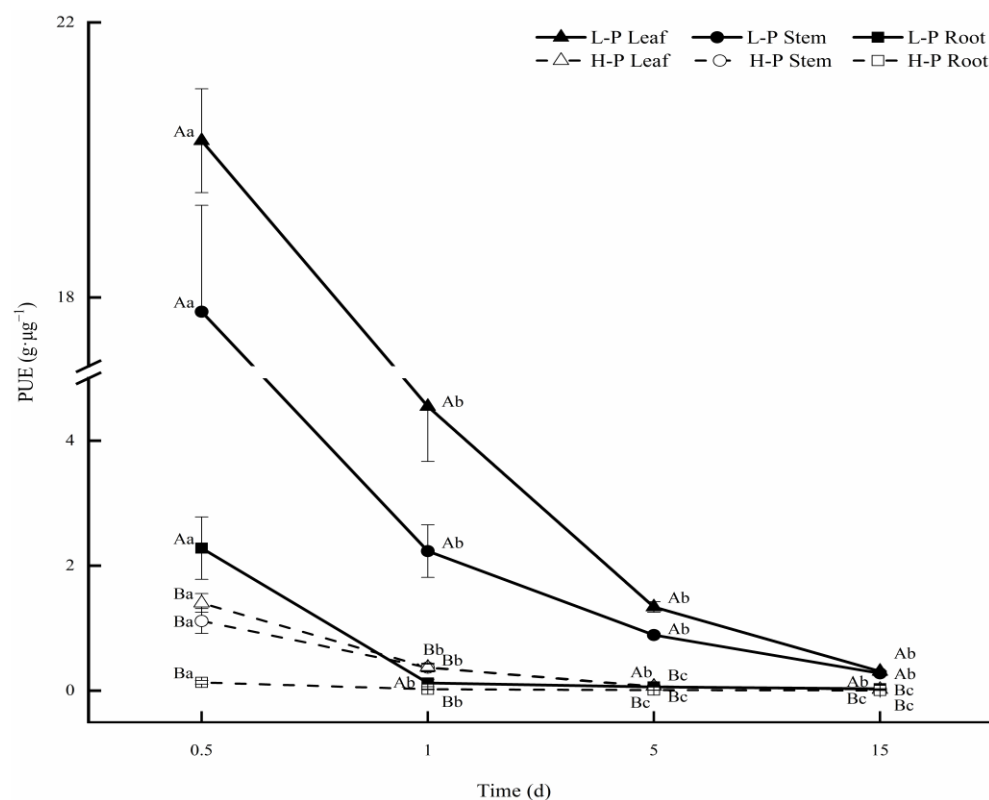
**Figure 7.** PUE in different organs under high- and low-P treatments. "L-P" and "H-P" represent the low-P and high-P treatments, respectively. Error bars represent standard errors, and each point in the figures represents the mean of the five replicates (*n* = 5). Lowercase letters indicate significant differences (*p* < 0.05) at different treatment times under the same P treatment. Uppercase letters indicate significant differences (*p* < 0.05) between different treatments at each time point.

### 3.7. Relationship between P Fractions and PUE in Different Organs

Correlation analysis between the different P fractions and PUE showed that the PUEs of the leaves and stems were both similarly negatively correlated with each P fraction, regardless of the P treatment (Table 1). Furthermore, the leaf PUE was significantly negatively correlated (*p* < 0.01) with inorganic P, ester P, and nucleic P under the low-P treatment. The correlations between the PUE and these three fractions in the stems were also significant (*p* < 0.05). However, the correlations between the PUE and the P fractions in the leaves and stems were not significant (*p* > 0.05) under the high-P treatment, except for ester P. In the roots, the PUE was significantly negatively correlated with nucleic P (*p* < 0.01) under the low-P treatment and significantly negatively correlated with ester P under the high-P treatment (*p* < 0.05).

**Table 1.** Correlations between P fractions and PUE in different organs.

| P Fractions | PUE for Dry Mass (g µg$^{-1}$) | | | | | |
| | Leaf | | Stem | | Root | |
| | L-P | H-P | L-P | H-P | L-P | H-P |
| --- | --- | --- | --- | --- | --- | --- |
| Inorganic P | −0.990 ** | −0.734 ns | −0.798 * | −0.701 ns | −0.018 ns | 0.661 ns |
| Ester P | −0.980 ** | −0.858 * | −0.816 * | −0.607 ns | 0.056 ns | −0.796 * |
| Lipid P | −0.720 ns | −0.772 ns | −0.642 ns | −0.723 ns | 0.440 ns | −0.623 ns |
| Nucleic P | −0.940 ** | −0.767 ns | −0.813 * | −0.785 ns | −0.878 ** | −0.549 ns |

ns Represents not significant with *p* > 0.05, * represents significant differences at *p* < 0.05, ** represents significant differences at *p* < 0.01; PUE represents P use efficiency, L-P and H-P represent the low-P and high-P treatments, respectively.

## 4. Discussion

It has been reported that plants can adjust the relative abundance of P in different fractions to improve nutrient utilization efficiency [10], as shown in herbaceous plants [12,18,19]. Our results investigating the M1 Chinese fir clone support the notion that it has the ability to redistribute and transfer P to different fractions, resulting in reduced P demand, maintaining aboveground productivity, and increasing root nutrient allocation in response to P limitations.

We found that the amount of the exogenous P absorbed by the M1 Chinese fir significantly decreased under the low-P treatment, which was caused by a reduction in P fractions and various P-containing biochemical compounds [7,12]. In contrast, the PUE under the low-P treatment was generally significantly higher than that under the high-P treatment across the analyzed time points and plant organs. This finding can also be explained by the P allocation patterns observed in our study, which showed that higher shoot-soluble P enhances P mobility and recycling, with large increases in the nucleic P observed in the roots, which are generally thought to be storage organs. We discuss this P allocation pattern in detail below.

In this study, we found that the total P in the leaves was significantly lower than that in the roots, and the PUE was highest in the leaves, followed by the stems and roots. It has been reported that plants generally reduce foliar P concentrations and enhance the PUE in response to low soil P availability [38]. An analysis of 340 tree and shrub species across various biomes found that the plants growing in P-poor soils increased the leaf toughness and leaf life span, thus allowing a greater P fraction to be allocated for metabolism rather than growth to maintain high PUE [12]. On the other hand, the M1 Chinese fir optimizes foliar P allocation for maintaining its productivity under limiting P conditions. The leaf PUE of M1 was significantly correlated with the abundance of inorganic P, ester P, and nucleic P under the low-P treatment. Inorganic P is expected to have higher resorption efficiency due to its high mobility [39]. In contrast, much more energy is required to degrade recalcitrant P compounds in senesced leaves to increase the P resorption efficiency in P-limited environments [40]. Our results showed that the ratio of soluble P (i.e., inorganic P and ester P) remained high in the leaves of M1 Chinese firs under the low-P treatment, while lipid P was lower than that under the high-P treatment. The proportion of nucleic P in the leaves also gradually increased under the low-P treatment, which may potentially limit productivity [39], similar to inorganic P. These findings showed that there was a relatively greater share of inorganic P and P-containing metabolites than other P fractions in the total P concentration. Lipid P showed lower content under the high-P supply, while the proportion of soluble P in the stems likely increased P mobility and improved the recycling capacity of P [10,30,41].

In contrast to the shoot and leaf patterns, inorganic P in the roots decreased over the course of the experiment, and ester P peaked at 1d in both treatment groups. The root's nucleic P was constant under high-P conditions but significantly increased with time under the low-P treatment. Studies of ecological stoichiometry have suggested that a great amount of nucleic P is in P-rich ribosomal RNA and that higher rates of plant growth require greater investment in ribosomal RNA to produce the proteins required for growth [42]. These findings can be explained by an increase in protein synthesis requiring higher P allocation to nucleic P; thus, higher root nucleic P may be a response to promote root growth to improve exogenous P absorption under P limitations. However, the soluble P content gradually decreased relative to insoluble P components under P limitations. We speculate that the P fractions in the roots were transferred. The plant absorption of P is strongly limited by exogenous P when the external P concentration is low, which ultimately limits plant growth [43]. To satisfy P demand for shoots, plants take up nutrients from the soil but also recycle nutrients internally through resorption and reallocation from storage organs (e.g., roots), which allows the reuse of nutrients for new growth [44–46]. It was also reported in *Hordeum vulgare* L. [30] that under low-P conditions, high-P-efficient

plants enhance the decomposition of ester P and nucleic P by increasing the activity of acid phosphatase in lower leaves so that newer, upper leaves can reuse their P.

In conclusion, the M1 Chinese fir shows a strong ability to optimize P allocation across P fractions and increase PUE to maintain its aboveground productivity in response to P limitations. In order to control the exogenous P supply accurately, hydroponics was used as the cultivation medium in this study. As we all know, the situation in the natural soil is extremely complex, and the absorption and utilization of P in plants are affected by other factors, such as the form of P [47], arbuscular mycorrhiza [48], the competitive utilization of P by rhizosphere microorganisms [49] and roots [22,50], the spatiotemporal heterogeneity of P in soil [51], etc. In view of most of these influencing factors, previous studies summarized the adaptation mechanism of the Chinese fir's response to P limitations [22,48,50,51]. For example, a higher PUE is partially explained by a mechanism that functions to transport cellular P to stems and leaves for reuse after inhibiting GA$_3$ and IAA [52] in root tips and promoting the dissolution of the root cortex to form aerenchyma [23]. Furthermore, plant secretions (i.e., H$^+$, total acid, oxalic acid, citric acid, etc.) [24,26] and the apoptosis of root cells could enhance the mobilization of insoluble rhizosphere P, thus improving the P uptake efficiency [53]. In addition, M1 showed higher yields under the low-P treatment than that under the high-P treatment, regardless of whether the cultivation medium was soil [21] or hydroponic. Based on previous research, in this study, we excluded the influence of other factors except for the amount of available P. Therefore, for future studies, researchers are recommended to investigate the mechanisms of P utilization and transport from the perspective of P fraction distribution under the influence of multiple factors, which will be closer to natural soil conditions.

## 5. Conclusions

We found that under limiting P conditions, the M1 Chinese fir clone reduced the allocation of exogenous P to leaves and stems and correspondingly increased its distribution to roots, in addition to generally reducing the total P concentration. However, the PUE of the different organs under the low-P treatment were all significantly higher than that observed under high-P treatment over the course of the experiment. PUE was generally significantly correlated with P fractions (i.e., inorganic P, ester P, and nucleic P), which showed that the higher PUE under the low-P treatment was explained by the net effect of a relatively greater share of metabolic P than structural P in the total P content. The M1 Chinese fir maintained a high ratio of soluble P (inorganic P and ester P) in its leaves and stems to increase P reuse capacity to adapt to low soil P availability. Our results suggest that P is transferred in the roots, as soluble inorganic P and ester P gradually decreased, while insoluble P components (e.g., nucleic P) accumulated in the roots to maintain a relatively stable root total P concentration. These responses likely facilitate root growth to increase exogenous P absorption under low-P conditions. We conclude that the M1 Chinese fir clone optimizes the allocation of P among P fractions (i.e., increases P mobility and recycling), reduces P demand (i.e., reduces total P concentration), and increases PUE to maintain its aboveground productivity in response to limited availability of P.

**Author Contributions:** Conceptualization, X.Z., L.C. and X.M.; methodology, S.C.; software, S.C.; validation, S.C., Q.L. and Z.H.; formal analysis, X.Z.; investigation, S.C.; resources, P.W.; data curation, S.C. and X.Z.; writing—original draft preparation, X.Z.; writing—review and editing, X.Z. and L.C.; visualization, S.C. and X.Z.; supervision, L.C.; project administration, X.Z., P.W. and X.M.; funding acquisition, X.Z., P.W. and X.M. All authors have read and agreed to the published version of the manuscript.

# References

1.  Lambers, H.; Brundrett, M.C.; Raven, J.A.; Hopper, S.D. Plant mineral nutrition in ancient landscapes: High plant species diversity on infertile soils is linked to functional diversity for nutritional strategies. *Plant Soil* **2011**, *348*, 7–27. [CrossRef]
2.  Ragothama, K.G.; Karthikeyan, A.S. Phosphate acquisition. *Plant Soil* **2005**, *274*, 37–49. [CrossRef]
3.  Fink, J.R.; Inda, A.V.; Bayer, C.; Torrent, J.; Barrón, V. Mineralogy and phosphorus adsorption in soils of south and central-west Brazil under conventional and no-tillage systems. *Acta Sci. Agron.* **2014**, *36*, 379–387. [CrossRef]
4.  Bortoluzzi, E.C.; Pérez, C.A.S.; Ardisson, J.D.; Tiecher, T.; Caner, L. Occurrence of iron and aluminum sesquioxides and their implications for the P sorption in subtropical soils. *Appl. Clay Sci.* **2015**, *104*, 196–204. [CrossRef]
5.  Freitas, E.C.S.D.; Paiva, H.N.D.; Leite, H.G.; Oliveira Neto, S.N.D. Effect of phosphate fertilization and base saturation of substrate on the seedlings growth and quality of *Plathymenia foliolosa* Benth. *Rev. Árvore* **2017**, *41*, e410111. [CrossRef]
6.  Lynch, J.P. Root phenes that reduce the metabolic costs of soil exploration: Opportunities for 21st century agriculture. *Plant Cell Environ.* **2014**, *38*, 1775–1784. [CrossRef]
7.  Veneklaas, E.J.; Lambers, H.; Bragg, J.; Finnegan, P.M.; Lovelock, C.E.; Plaxton, W.C.; Price, C.A.; Scheible, W.R.; Shane, M.W.; White, P.J.; et al. Opportunities for improving phosphorus-use efficiency in crop plants. *New Phytol.* **2012**, *195*, 306–320. [CrossRef]
8.  Huang, C.Y.; Shirley, N.; Genc, Y.; Shi, B.; Langridge, P. Phosphate utilization efficiency correlates with expression of low-affinity phosphate transporters and noncoding RNA, IPS1, in Barley. *Plant Physiol.* **2011**, *156*, 1217–1229. [CrossRef]
9.  Hammond, J.P.; Broadley, M.R.; White, P.J.; King, G.J.; Bowen, H.C.; Hayden, R.; Meacham, M.C.; Mead, A.; Overs, T.; Spracklen, W.P.; et al. Shoot yield drives phosphorus use efficiency in *Brassica oleracea* and correlates with root architecture traits. *J. Exp. Bot.* **2009**, *60*, 1953–1968. [CrossRef]
10. Shi, L.; Liang, H.L.; Xu, F.S.; Wang, Y.H. Genotypic variation in phosphorus fractions and its relation to phosphorus efficiency in seedlings of *Brassica napus* L. *Plant Nutr. Fert. Sci.* **2008**, *14*, 351–356. [CrossRef]
11. Rouached, H.; Stefanovic, A.; Secco, D.; Arpat, A.B.; Gout, E.; Bligny, R.; Bligny, R.; Poirier, Y. Uncoupling phosphate deficiency from its major effects on growth and transcriptome via *PHO1* expression in *Arabidopsis*. *Plant J.* **2011**, *65*, 557–570. [CrossRef]
12. Hidaka, A.; Kitayama, K. Allocation of foliar phosphorus fractions and leaf traits of tropical tree species in response to decreased soil phosphorus availability on Mount Kinabalu, Borneo. *J. Ecol.* **2011**, *99*, 849–857. [CrossRef]
13. Piccin, R.; Couto, R.D.R.; Bellinaso, R.J.S.; Gatiboni, L.C.; Conti, L.D.; Rodrigues, L.A.T.; Somavilla, L.M.; Brunetto, G. Phosphorus forms in leaves and their relationships with must composition and yield in grapevines. *Pesqui. Agropecu. Bras.* **2017**, *52*, 319–327. [CrossRef]
14. Kulmann, M.S.S.; Stefanello, L.O.S.; Schwalbert, R.A.; Berghetti, L.L.P.; Brunetto, G. Effects of phosphorus fertilizer application on phosphorus fractions in different organs of *Cordia trichotoma*. *J. For. Res.* **2020**, *32*, 725–732. [CrossRef]
15. Elser, J.; Bennett, E. Phosphorus cycle: A broken biogeochemical cycle. *Nature* **2011**, *478*, 29–31. [CrossRef] [PubMed]
16. Wieneke, J. Phosphorus efficiency and phosphorus remobilization in two sorghum (*Sorghum bicolor* (L.) Moench) cultivars. *Plant Soil* **1990**, *123*, 139–145. [CrossRef]
17. Moro, H.; Park, H.D.; Kunito, T. Organic phosphorus substantially contributes to crop plant nutrition in soils with low phosphorus availability. *Agronomy* **2021**, *11*, 903. [CrossRef]
18. Mayers, X.G.; Turner, B.L.; Laliberté, E. Greater root phosphatase activity of tropical trees at low phosphorus despite strong variation among species. *Ecology* **2020**, *101*, e03090. [CrossRef]
19. Wang, F.C.; Fang, X.M.; Wang, G.G.; Rong, M.; Lin, X.F.; Wang, H.M.; Chen, F.S. Effects of nutrient addition on foliar phosphorus fractions and their resorption in different-aged leaves of Chinese fir in subtropical China. *Plant Soil* **2019**, *443*, 41–54. [CrossRef]
20. Fan, S.H.; Shen, W.T.; Ma, X.Q.; Lin, K.M.; Zhang, X.Q. Effect of successive planting on productivity of Chinese fir of different age plantations. *For. Res.* **2003**, *16*, 560–567. [CrossRef]
21. Wu, P.F. Adaptation Mechanism of Chinese Fir Clones with High Phosphorus-Use-Efficiency to Envrironmental Phosphorus Stress. Ph.D. Thesis, Fujian Agriculture and Forestry University, Fuzhou, China, 2009.

22. Wu, P.F.; Wang, G.Y.; Farooq, T.H.; Li, Q.; Zou, X.H.; Ma, X.Q. Low phosphorus and competition affect Chinese fir cutting growth and root organic acid content: Does neighboring root activity aggravate P nutrient deficiency? *J. Soils Sediments* **2017**, *17*, 2775–2785. [CrossRef]

23. Wu, P.F.; Lai, H.Y.; Mulualem, T.; Wu, W.; Wang, P.; Wang, G.Y.; Ma, X.Q. Does phosphorus deficiency induce formation of root cortical aerenchyma maintaining growth of *Cunninghamia lanceolata*? *Trees* **2018**, *32*, 1633–1642. [CrossRef]

24. Zou, X.H.; Wei, D.; Wu, P.F.; Zhang, Y.; Hu, Y.N.; Chen, S.T.; Ma, X.Q. Strategies of organic acid production and exudation in response to low-P stress in Chinese fir genotypes differing in P-use efficiencies. *Trees* **2018**, *32*, 897–912. [CrossRef]

25. Chen, W.T.; Zhou, M.Y.; Zhao, M.Z.; Chen, R.H.; Mulualem, T.; Wu, P.F.; Li, M.; Ma, X.Q. Transcriptome analysis provides insights into the root response of Chinese fir to phosphorus deficiency. *BMC Plant Biol.* **2021**, *21*, 525. [CrossRef]

26. Lai, H.Y.; Wu, K.; Wang, N.M.; Wu, W.J.; Wu, P.F. Relationship between volatile organic compounds released and growth of *Cunninghamia lanceolata* roots under low-P conditions. *iForest* **2018**, *11*, 713–720. [CrossRef]

27. Liang, X.; Liu, A.Q.; Ma, X.Q.; Feng, L.Z.; Chen, Y.L. The effect of phosphorus deficiency stress on activities of acid phosphatase in different clones of Chinese fir. *Chin. J. Plant Ecol.* **2005**, *29*, 54–59. [CrossRef]

28. Zou, X.H. The Different Stages Response and its Signal Regulation of Different Chinese Fir with Different P-Use Efficiency to Low-Phosphorus Stress. Ph.D. Thesis, Fujian Agriculture and Forestry University, Fuzhou, China, 2018.

29. Tian, J.; Wang, X.R.; Tong, Y.P.; Chen, X.P.; Liao, H. Bioengineering and management for efficient phosphorus utilization in crops and pastures. *Curr. Opin. Biotech.* **2012**, *23*, 866–871. [CrossRef]

30. Liu, T.; Chen, H.Y.; Yu, H.Y.; Li, T.X.; Gao, S.Q.; Chen, G.D. Characterization of phosphorus utilization in Barley leaf under low phosphorus stress. *Chin. Bull. Bot.* **2016**, *51*, 504–514. [CrossRef]

31. Feike, A.D.; He, M.; Johansen, M.P.; Jennifer, J.H.; Claudia, K. Plant and microbial uptake of nitrogen and phosphorus affected by drought using $^{15}$N and $^{32}$P tracers. *Soil Biol. Biochem.* **2015**, *82*, 135–142. [CrossRef]

32. Mildaryani, W.; Mujiyo, M.; Dewi, W.S.; Poernomo, D. Isotopic tracing of phosphorus uptake in Oil Palm seedlings leaf axil using $^{32}$P labelled. *Int. J. Adv. Sci. Eng. Inf. Tech.* **2020**, *10*, 368–373. [CrossRef]

33. Sheng, W.T.; Fan, S.H. Soil changes of Chinese fir plantation. In *Long-Term Productivity of Chinese Fir Plantations*; China Science Publishing: Beijing, China, 2005; pp. 78–80.

34. Wu, P.F.; Ma, X.Q.; Mulualem, T.; Wang, C.; Liu, A.Q.; Odén, P.C. Root morphological plasticity and biomass production of two Chinese fir clones with high phosphorus efficiency under low phosphorus stress. *Can. J. For. Res.* **2011**, *41*, 228–234. [CrossRef]

35. Howard, G. The early history of $^{32}$P as a radioactive tracer in biochemical research. *Biochem. Mol. Biol. Edu.* **2005**, *33*, 159–164. [CrossRef]

36. Kedrowski, R.A. Extraction and analysis of nitrogen, phosphorus and carbon fractions in plant material. *J. Plant Nutr.* **1983**, *6*, 989–1011. [CrossRef]

37. Nurmayulis, N.; Citraresmini, A.; Anas, I. The use of $^{32}$P method to evaluate the growth of lowland rice cultivated in a system of rice intensification (SRI). *At. Indones.* **2013**, *39*, 88. [CrossRef]

38. Yang, X.L.; Liu, Y.X.; Wu, F.K.; Jiang, X.J.; Yu, L.; Wang, Z.Q.; Zhang, Z.L.; Ma, J.; Chen, G.D.; Wei, Y.M.; et al. Quantitative trait loci analysis of root traits under phosphorus deficiency at the seedling stage in wheat. *Genome* **2018**, *61*, 209–215. [CrossRef] [PubMed]

39. Tsujii, Y.; Onoda, Y.; Kitayama, K. Phosphorus and nitrogen resorption from different chemical fractions in senescing leaves of tropical tree species on Mount Kinabalu, Borneo. *Oecologia* **2017**, *185*, 171–180. [CrossRef]

40. Hidaka, A.; Kitayama, K. Relationship between photosynthetic phosphorus-use efficiency and foliar phosphorus fractions in tropical tree species. *Ecol. Evol.* **2013**, *3*, 4872–4880. [CrossRef]

41. Mo, Q.F.; Li, Z.A.; Sayer, E.J.; Lambers, H.; Li, Y.; Zou, B.; Tang, J.W.; Heske, M.; Ding, Y.Z.; Wang, F.M. Foliar phosphorus fractions reveal how tropical plants maintain photosynthetic rates despite low soil phosphorus availability. *Funct. Ecol.* **2019**, *33*, 503–513. [CrossRef]

42. Perkins, M.C.; Woods, H.A.; Harrison, J.F.; Elser, J.J. Dietary phosphorus affects the growth of larval *Manduca sexta*. *Arch. Insect Biochem. Physiol.* **2004**, *55*, 153–168. [CrossRef]

43. Yuan, Z.Y.; Chen, H. Negative effects of fertilization on plant nutrient resorption. *Ecology* **2015**, *96*, 373–380. [CrossRef]

44. Valverde-Barrantes, O.J.; Gregoire, T.F.; Roumet, C.; Blackwood, C.B. A worldview of root traits: The influence of ancestry, growth form, climate and mycorrhizal association on the functional trait variation of fine-root tissues in seed plants. *New Phytol.* **2017**, *215*, 1295–1297. [CrossRef] [PubMed]

45. Klimeová, M.; Rindi, F.; Kaloud, P. There is more than meets the eye: DNA cloning demonstrates high genetic heterogeneity in populations of the subaerial green alga *Trentepohlia* (*Trentepohliales, Chlorophyta*). *J. Phycol.* **2018**, *55*, 224–235. [CrossRef] [PubMed]

46. Wang, R.; Cresswell, T.; Johansen, M.P.; Harrison, J.J.; Jiang, Y.; Keitel, C.; Cavagnaro, T.R.; Dijkstra, F.A. Re-allocation of nitrogen and phosphorus from roots drives regrowth of grasses and sedges after defoliation under deficit irrigation and nitrogen enrichment. *J. Ecol.* **2021**, *109*, 4071–4080. [CrossRef]

47. Meyer, G.; Bell, M.J.; Doolette, C.L.; Brunetti, G.; Zhang, Y.Q.; Lombi, E.; Kopittke, P.M. Plant-Available Phosphorus in Highly Concentrated Fertilizer Bands: Effects of Soil Type, Phosphorus Form, and Coapplied Potassium. *J. Agric. Food Chem.* **2020**, *29*, 7571–7580. [CrossRef] [PubMed]

48. Cao, Y.; Li, N.N.; Lin, J.Q.; Zhang, Y.; Ma, X.Q.; Wu, P.F. Root system-rhizosphere soil-bulk soil interactions in different Chinese fir clones based on fungi community diversity change. *Front. Ecol. Evol.* **2022**, *10*, 1028686. [CrossRef]

49. Peng, Y.; Duan, Y.S.; Huo, W.G.; Zhang, Z.J.; Huang, D.; Xu, M.G.; Wang, X.H.; Yang, X.Y.; Wang, B.R.; Kuzyakov, Y.; et al. C:P stoichiometric imbalance between soil and microorganisms drives microbial phosphorus turnover in the rhizosphere. *Biol. Fert. Soils* **2022**, *58*, 421–433. [CrossRef]
50. Muhammad, H.U.R.; Guo, H.L.; Zheng, S.S.; Li, L.X.; Ma, X.Q.; Taimoor, H.F.; Muhammad, F.N.; Narayan, P.G.; Wu, P.F. Effects of low phosphorus availability on root cambial activity, biomass production and root morphological pattern in two clones of Chinese fir. *Forestry* **2022**, cpac030. [CrossRef]
51. Zou, X.H.; Wu, P.F.; Chen, N.L.; Wang, P.; Ma, X.Q. Chinese fir root response to spatial and temporal heterogeneity of phosphorus availability in the soil. *Can. J. For. Res.* **2015**, *45*, 402–410. [CrossRef]
52. Zou, X.H.; Hu, Y.N.; Wei, D.; Chen, S.T.; Wu, P.F.; Ma, X.Q. Correlation between endogenous hormone and the adaptability of Chinese fir with high phosphorus-use efficiency to low phosphorus stress. *Chin. J. Plant Ecol.* **2019**, *43*, 139–151. [CrossRef]
53. Wu, P.F.; Wang, G.Y.; El-Kassaby, Y.A.; Wang, P.; Zou, X.H.; Ma, X.Q. Solubilization of aluminum-bound phosphorus by root cell walls: Evidence from Chinese fir, *Cunninghamia lanceolata*. *Can. J. For. Res.* **2017**, *47*, 419–423. [CrossRef]